Robotica (2017) volume 35, pp. 143–165. © Cambridge University Press 2015
doi:10.1017/S0263574715000041

Perceptive communicating capsules for fluid flow measurement and visualisation

Robert Logan Stewart†*, Ilija Denis Šutalo† and Petar Liovic‡

†*Fluid Dynamics Group, Manufacturing Flagship, CSIRO (Commonwealth Scientific and Industrial Research Organisation), Highett, VIC, 3190, Australia*
‡*Mineral Resources Flagship, CSIRO, Clayton, VIC, 3168, Australia*

(Accepted January 5, 2015. First published online: February 18, 2015)

SUMMARY
A new approach to flow measurement and visualisation in fluid dynamics based on a group of perceptive communicating capsules has been developed. Experiments were carried out with fluid-mobilised and stationary capsules deployed in a fluid flow test rig (raceway pond). Each capsule contains a microcontroller, battery, infra-red and visible LEDs and other electronics. Using optical communications, capsules can record encounters with one another. From the resulting interaction patterns, fluid flow speed and path-frequency measurements were obtained. Additionally, the capsules have shown the capacity for distributed sensing, and their streaklines provide a valuable means of external visualisation.

1. Introduction

1.1. Flow measurement and visualisation

Numerous techniques are used for the flow measurement and flow visualisation in complex geometries.[1,2] To name just a few, some examples include: particle imaging velocimetry (PIV),[3] laser Doppler velocimetry,[4] streak photography,[5] the use of dye or tracer particles,[6,7] electrical capacitance tomography[8] and ultrasound velocity profiling.[9] Experimental measurement and visualisation techniques are used to understand the dynamics of fluid flow and to validate the theoretical predictions and computational fluid dynamics (CFD) models. An ideal measurement system would allow the fluid velocity flow field to be quantified in the three spatial dimensions as a function of time. Other properties of interest (e.g., pressure, temperature, pH and chemical concentrations) may also be required for a comprehensive understanding of a system.

Despite the many available techniques, each has limitations that restricts its applicability to certain niche scenarios. For instance, the flow measurement and visualisation systems may be too invasive, expensive or complex to set-up, be wasteful of resources, require specialist training to use, be impractical for use *in situ*, have a limited interrogation area/volume, or be unable to measure physical quantities of interest. In addition, certain fluids may not be amenable to analysis with a chosen technique due to the inherent properties of the fluid. For example, the fluid in a system may absorb externally applied ultrasound or light radiation to such a degree that detectors using these modalities cannot be used. There is still a need, therefore, for the development of new flow measurement techniques that overcome these limitations and provide alternative means for observing a system. In developing the novel flow measurement techniques, there is an opportunity to gain a new understanding that can lead to outstanding problems in fluid dynamics being solved.

In this paper, a new flow measurement and visualisation system is proposed that consists of a group of perceptive communicating capsules. It is envisaged that the techniques developed will find application in industry and in the field (e.g. in measuring river, pipeline and sewer flows).

* Corresponding author. E-mail: RLStewart@ieee.org

In the next section (Section 1.2), we explore some of the new technologies that are relevant to the novel flow measurement and visualisation approach detailed in this paper.

1.2. Systems of multiple intelligent entities: Sensor networks, reconfigurable robots and robotic swarms

Recent advances in microelectronics and miniaturisation have allowed new sensing and robotic techniques to be developed. Lower part costs have meant that distributed systems composed of large numbers of individually intelligent parts can now be developed inexpensively, giving rise to new applications and measurement approaches.

The development of sensor networks is one example that has benefited from such advances. Sensor networks are wireless communication networks that are composed of multiple sensor nodes (often called motes). These nodes are distributed in an environment to perform sensing spatially over a region. The vision of having some "smart-dust", comprising thousands of cubic-millimetre sized sensors[10] that could be scattered in an environment to perform sensing, has provided a futuristic goal and some impetus to the sensor network area. Sensor networks have been proposed for applications in areas such as: environmental monitoring,[11] pipeline monitoring,[12] tracking of plant/animal movements,[10,13] agriculture,[14] structural health monitoring[15]and health-care monitoring in smart homes.[16,17] Much of the research to date has focused on solving problems related to communication network routing, reliability, security and privacy, energy efficiency, data management and localisation amongst fixed nodes (although, mobile robotic nodes are also being considered).[18–22]

In the field of robotics, technology advances have also given rise to systems that are composed of large numbers of intelligent autonomous entities. For example, modular robotic systems are being developed that are able to change their morphology for a specific task or type of locomotion.[23–25] Modules usually maintain connectivity with each other as they move, although this is not always the case. "Pebble" modules (cubes with 12 mm sides) have been designed as a step towards "programmable matter"—modules able to form into objects, such as tools, on demand.[26] Self-assembling "programmable parts" have also been detailed,[27] where modules floating on an air-table are able to connect to one another and assemble into different shapes such as triangles and hexagons. Along similar lines, stochastic assembly of modules (with 15 mm length) has been demonstrated in a flow tank.[28] In the system detail, 3D target structures can be assembled on an "active assembly substrate" which has an array of valves that change the fluid flow and allow control over the modules.

Swarm robotics is another related area of robotics research that involves the creation of robotic systems composed of many autonomous parts. Research in this area is inspired by social insects (ants, bees, wasps and termites), and the collective or swarm intelligence that emerges from the individuals in a colony (refer to ref. [29]). The emphasis in swarm robotics is on developing mobile and decentralised systems that are composed of many simple autonomous robots. These robots achieve coordination by interacting locally, through direct and indirect forms of communication. Numerous problem domains/applications have been investigated in swarm robotics. A few examples include: box pushing,[30] foraging,[31] collective construction,[32,33] leaf curling[34] and self-assembly.[35]

For a robot swarm to perform its global task/s in the absence of a centralised global control, often a means of assessing global information through local means is required. For example, in a collective construction task where robots are building a large structure, they can indirectly assess the global state of assembly using local cues, such as the presence/absence of blocks in certain locations or with specific markings.[32,36] Other examples where the global properties or state of a system are estimated by robots through local means include: the measurement of area,[37,38] global position estimation through "social odometry",[39,40] and in estimating global consensus for colony-level decisions.[41]

1.3. Perceptive communicating capsules

Can recent distributed approaches to sensing and robotics as discussed above find utility in the study of fluid dynamics? In this paper, we propose and demonstrate a proof-of-concept for a new flow measurement and visualisation system that involves the use of a group of 12 perceptive capsules. The capsules are shown in Fig. 1 along with a control box for capsule initialisation and data retrieval. As will be discussed in detail later, the capsules are spherical (with 28 mm diameter), and each contains a battery, a microcontroller, infra-red receiver-transmitter for close range optical

Fig. 1. Photograph of the group of 12 capsules and a control box that interfaces to a PC via a serial link. Each capsule has its LED switched on.

communications[1], ambient light sensor and coloured LED for external visualisation and user feedback. Their functionality is intentionally minimalist. The capsules can be sealed and are able to operate in a relatively harsh fluidic environment (e.g. in the presence of a rotating impeller) and their mass can be manually adjusted to allow changes in buoyancy. They are able to be inserted into a flow, so they become fluid-mobilised, or fixed as designated stationary nodes.

Small electronic and radio frequency (RF) capsules have already been developed by other researchers for medical use in the human body or tracking/tagging of animals.[42,43] In many cases, capsules are able to be injected or swallowed. Robotic capsules able to be steered inside the body through external means are also being created,[44–48] and applications abound for tiny robots able to operate inside the human body.[49]

Larger scale robots have been built for studying oceanographic systems, such as AUVs (Autonomous Underwater Vehicles), buoys, gliders and drifters.[50–52] These devices, once deployed, can be tracked and used to provide data that can be combined to inform a picture of ocean currents or other properties of interest.

Relatively few small-scale robot systems have been developed purposefully for studying fluid flow and most examples target specific applications. In ref. [53], a system is detailed for studying coastal erosion, that allows natural pebbles with embedded RFID tags to be identified and their paths traced somewhat manually. A mobile sensor network has been reported in ref. [54] for pipeline monitoring with capsular nodes equipped with arms for attaching to the wall inside a pipe. These nodes are relatively sophisticated and are equipped with radio communications and gyroscopes. In refs. [55]–[56] a "smart sediment pebble" is described for studying sediment transport in river beds, that is capable of tracking its 3D trajectory using gyroscopes and accelerometers. Our capsules, which are also spherical, resemble this synthetic "pebble" in shape but are purposefully much simpler in their individual functionality. Their minimalist design should allow further miniaturisation and a scaling up of the number of capsules in a system.

Whilst it would possibly also be beneficial to integrate accelerometers and gyroscopes into our capsules, we are interested in finding out to what degree interactions alone are sufficient for determining properties of the global flow field. In social insect colonies, interactions can convey useful information about the state of a colony. For example, encounter rate may indicate which tasks an insect's co-workers are doing and help inform the insect what it should therefore be doing.[57,58]

[1] It should be possible to additionally add RF communication (e.g. Bluetooth or Wi-Fi) capabilities to the capsules. However, for the initial design we decided to employ close range optical communications to avoid potential problems associated with transmitting radio waves within fluids and to permit use of the capsules in industrial set-ups requiring operation within metallic pipes or vessels.

Encounter rate can also help insects in quorum sensing during emigration where the best of a number of candidate nest sites needs to be determined by the colony[59]—this has inspired techniques for collective decision making in multi-robot systems.[41] These examples suggest that it is possible to measure certain global properties of a system by simply looking at the patterns of encounters between individuals. We hypothesise that by recording encounters between capsules and then performing offline analysis of recorded data, velocity flow field data may be measured.

It should be stressed that the capsules that have been developed are mobilised by the fluid flow and currently do not possess self-mobility or actuation, so we stop short of calling them robots. Additionally, the capsules do not process nor significantly act upon their perceptions, so do not really possess a swarm intelligence. However, the information gathering approach is inspired by mechanisms of information transfer observed in social insect colonies, and can apply to a group composed of robots that do have self-mobility and actuators. Whether 12 capsules can be called a swarm is debatable. Whilst insect colonies can range from a handful of individuals to millions,[60] we take a conservative view and refer to the 12 capsules developed as a *group* rather than a *swarm*. However, if the number of capsules was scaled up to hundreds as envisaged, the term *swarm* would be more apt.

This paper provides a preliminary investigation into the use of capsule encounters as a means to revealing a global picture of the fluid flow in a system. Additionally two other applications (namely, streamline visualisation and distributed sensing) are also detailed that will have immediate practical use to the fluid dynamics research community. Using a group of minimalist capsules is a fundamental point of difference from other fluid-flow measurement systems. The capsules that are detailed will be useful in helping the fluid dynamics researchers to better understand flow systems and to validate CFD models and theoretical predictions.

The remainder of this paper is structured as follows. In Section 2, we detailed the system that has been designed and provide details of both the hardware and software. In Section 3, an example case study of a raceway pond system is introduced and three different applications (speed measurements through encounters, distributed sensing and streamline visualisation) are demonstrated for the capsules through a number of experimental trials. Section 4 then highlights the many possible directions for future work arising out from the group of capsules developed. Finally, conclusions are presented in Section 5.

2. System Design

2.1. System overview

The flow measurement and visualisation system that was designed and developed comprised a group of 12 capsules and a control box that was interfaced to a computer via a serial link (refer to Fig. 1). A custom-made software application on the computer was used for initialising the capsules prior to an experiment, and retrieving data from the capsules after an experiment. It also provided an interface for directly communicating with capsules and controlling their functionality.

2.2. Hardware design

For the fluid flow measurements, it was important that the capsules be small and of adjustable buoyancy, so they could follow the fluid flow streamlines without significantly influencing the flow being measured. For a prototype system, transparent and hollow plastic capsules were used that were approximately spherical in shape, with an outer diameter of ∼28 mm. Smaller capsules could be used in the future to try and approach the ideal of a point particle with zero mass but, for manual assembly and prototyping, this size was convenient. Each capsule was composed of two hemispheres that fitted together in a lap joint arrangement. To ensure a water-tight seal, prior to use, thread seal tape was wrapped around the mating surface of one hemisphere before pressing the two halves of a capsule together.

Each capsule housed an electronic system designed for recording encounters and sensor data. The main electronic components were: an 8-bit microcontroller (Atmel ATMEGA 168PA with 16kB flash memory, 512B EEPROM and 1kB RAM), infra-red emitting diode (Vishay TSUS5202), infra-red receiver module (Vishay TSOP4836), a coloured LED (yellow, orange, red, green or blue) for visual feedback, a phototransistor ambient light sensor, a six-way socket for microcontroller

https://doi.org/10.1017/S0263574715000041 Published online by Cambridge University Press

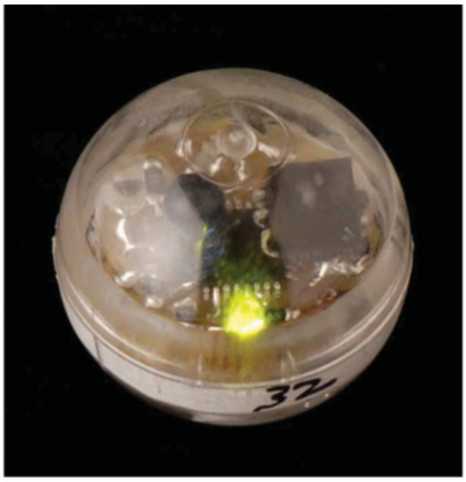

(a) Oblique view of a capsule.

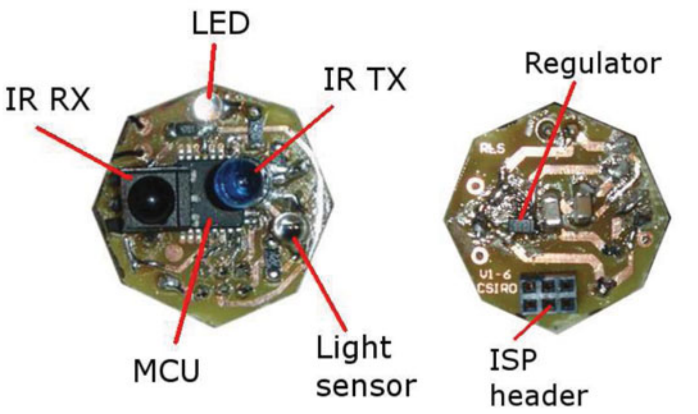

(b) Top view of PCB. (c) Bottom view of PCB.

Fig. 2. A close-up photograph of a capsule with a green LED is shown in (a). White thread seal tape can be seen around the capsule's centre and the battery is housed in the bottom hemisphere of the capsule. The top and bottom views, in (b) and (c) respectively, of a capsule's populated PCB are shown with the main components labelled.

in-system-programming (ISP), a 2.7 V regulator and a 3 V battery (CR2032 type). Rather than using a crystal oscillator, to save space, the microcontroller's internal RC oscillator was used as a clock signal at the expense of some accuracy. A photograph of a capsule is given in Fig. 2(a), and a capsule's printed circuit board (PCB) with components fitted is shown in Figs. 2(b) and (c).

The control box followed a similar design to the capsules with an ATMEGA 168PA microcontroller and infra-red receive-transmit (IR Rx-Tx) functionality to allow it to communicate with the capsules. Additionally, the control box also had an RS232 serial transceiver so it could be connected to the serial port of a laptop/desktop computer and controlled from high-level application software. A crystal oscillator was used for increased clock accuracy since, in this case, PCB space was plentiful. The clock signal was used by the microcontroller in the control box to create a relatively accurate timer that capsule timers could be synchronised to at the start of an experiment.

The PCBs for the control box and capsules were designed using Altium Designer and etched "in-house". The boards were octagonal in shape (with a side length $\approx$9.2 mm) to aid manufacture, since boards of this shape could readily be cut and filed to size manually compared to a preferable circular design. Parts were manually soldered onto the PCBs and each populated board was fitted into a capsule hemisphere and secured in place using hot glue. A 3V battery for a capsule was stuck to the

S	Instruction	ID	Data	CRC
2b	8b	8b	12b	4b

Fig. 3. Diagram showing the format for the 34-bit communication packet sent between capsules and between capsules and the control box. The packet contains 2 start bits (labelled S), an 8-bit instruction code, 8-bit ID code, 12-bits of data and a 4-bit CRC code.

bottom of the PCB along with additional weight (e.g. metallic washers), where required, to achieve a desired mass.

Each capsule was relatively inexpensive to make, with the electronic parts and one non-rechargeable battery for a capsule costing under A$20 (per item rate based on pricing for construction of 10 capsules). With larger volumes, this cost could be significantly reduced. Preference was given to RoHS (restriction of hazardous substances directive) compliant parts when purchasing parts not already in existing supplies. For future designs, rechargeable batteries could be used to minimise wastage and the ongoing costs of replacing batteries.

2.3. Software design

2.3.1. Microcontroller code. The code for the microcontrollers was developed in C and assembler using AVR Studio, and WinAVR (which includes the avr-gcc compiler). Each capsule microcontroller was programmed with the generated HEX file through its ISP header using an AVRISP mkII programming device.

The capsules were programmed to be able to receive and transmit data packets using optical infra-red communications. For simplicity, it was decided that a communications protocol similar to that found in hand-held remote control units would be used. The Phillips RC5 coding scheme, for which Atmel provides application notes[61,62] and routines for transmission and reception on their website[2], was adapted for our work. For transmission in this scheme, Manchester/bi-phase encoded bits are modulated by a carrier and the signal used to drive an infra-red emitter. For reception, a capsule's remote control receiver module outputs a demodulated signal. This signal is read by the microcontroller and decoded.

A custom-designed 34-bit packet format was chosen (shown in Fig. 3), departing from the 14-bit packet used for the RC5 protocol. The packet consists of two start bits, an instruction byte, an ID byte that identifies the capsule that the message is intended for (when the target ID is known), 12-bits of instruction dependent data and 4-bits for a cyclic redundancy check (CRC) code. If the integrity of a packet is confirmed (by computing a valid CRC), an action in response to the message can be taken. It is important to highlight that the capsules are capable of bi-directional communications. This is different from a standard television infra-red remote control unit which typically only sends commands *to* a television and does not receive commands *from* a television. The duration of sending one packet is approximately 60 ms.

A transmission that is initiated by a capsule or the base station will have an instruction byte indicating the packet is a *request*. In reply, an answering capsule will send a corresponding *response* instruction byte and any data that was requested. One exception to this strategy is a "broadcast ID" message that a capsule can transmit to tell neighbouring capsules it is nearby. This particular message does not expect a reply.

A collection of *request-response* messages, that allowed fetch and set operations, were implemented to provide control over the capsule's functionality as well as access to data. Attributes that could be set/fetched include a capsule's:

- ID value;
- timer value;
- data values (fetched or cleared only);
- sensor value (fetched only);
- LED mode (e.g. *on*, *off*, *on during transmit*, *on at a certain time*);
- capsule operation mode (namely: *Mobile-Tx-Rx*, *Stationary-Rx*, *Mobile-Sensing* or *Idle*);
- IR transmit strength.

[2] http://www.atmel.com/

https://doi.org/10.1017/S0263574715000041 Published online by Cambridge University Press

The capsules could be put into a number of different modes by changing the *capsule operation mode* parameter listed above. Each mode had a specific functionality and control structure. For the trials detailed in this paper, the capsules were programmed to have four modes of operation:

- *Mobile-Tx-Rx*: Operation as a fluid-mobilised capsule that periodically broadcasts its own ID and records the IDs of transmitting capsules and time of detection;
- *Stationary-Rx*: Operation as a fixed capsule that remains stationary and records IDs of transmitting capsules and time of detection;
- *Mobile-Sensing*: Operation as a fluid-mobilised capsule that performs sensing, periodically recording measurements from its ambient light sensor;
- *Idle*: Waiting for a packet[3].

2.4. Software application for high-level control

To test, initialise and retrieve data from the capsules, a PC software application was developed. The application was programmed in C# under Microsoft Visual Studio 2008 and used the Microsoft .NET Framework (version 3.5). The software application communicated via a serial link with the control box (refer to Fig. 1) that in turn optically communicated with capsules. A graphical user interface (GUI) provided easy user access for control over a capsule's functionality which was useful for testing. Additionally, the functionality of the control box itself could also be controlled from the software application. For example, the control box could be made to broadcast an arbitrary ID or have its timer value fetched/set.

The software application provided a means for initialising capsules before a trial and then retrieving data from the capsules after a trial. To do this, routines were programmed that consisted of a series of low-level commands. For example, before a trial, the control box's timer was reset and then each capsule was initialised in turn by: being given an unique ID, having its timer approximately synchronised with the master timer, having its data cleared and being put into a specific mode for the trial. After a trial was complete, the software application allowed data to be retrieved from the capsules and saved to file for post-experiment analysis.

3. Example Case Study: Investigating the Fluid Flow in a Raceway Pond

3.1. Study context and experimental set-up

To demonstrate the utility of the capsules for the measurement of fluid flow, a small-scale "raceway" pond system was investigated as an example of case study. A raceway pond, so-called because it resembles a raceway, is a closed-loop shallow channel that is powered by a paddle wheel.[63] Raceway ponds are used in the farming of algae. In such ponds, water, nutrients and algae are circulated by a paddle wheel that allows mixing of the nutrients and carbon dioxide (see ref. [64]). The design of energy-efficient raceway ponds is the subject of on-going theoretical and practical interest.

A small-scale version of a raceway pond provided an interesting experimental test-bed for trialling the capsules. The raceway pond rig was an uncovered system allowing external observation of the fluid (e.g. via a camera). We note, however, that in the future it is intended that the capsules be used within enclosed systems, where external observation is not possible/feasible. Figure 4(a) shows a photograph of the experimental test rig that was used for the experiments documented in this paper. A diagrammatic overhead view of the set-up is given in Fig. 4(b) with the position of an 8-blade paddle wheel indicated. The raceway pond had a deep and shallow end and an island baffle. A more detailed description of the raceway pond design is given elsewhere (see ref. [65]).

The paddle wheel was driven by a belt drive coupled to a motor that turned so as to circulate fluid clockwise (when viewed from above, in Fig. 4(b)). A custom-made tachometer was used to measure the paddle wheel speed in the experiments[4]. The paddle wheel was set to a height so that the minimum

[3] As the capsules do not receive commands while they are transmitting (e.g. in the *Mobile-Tx-Rx* mode), messages may need to be re-transmitted before they are successfully received. Therefore, after a trial, capsules were put into the *Idle* mode before uploading data so as to increase throughput.

[4] A small rare-earth magnet was mounted on one of the paddle wheel blades and arranged to close a reed-switch mounted on the wall of the tank at every rotation of the paddle wheel. The signal from the reed-switch was de-bounced using standard electronic techniques and fed into an oscilloscope (Rigol DS5062MA), where the

https://doi.org/10.1017/S0263574715000041 Published online by Cambridge University Press

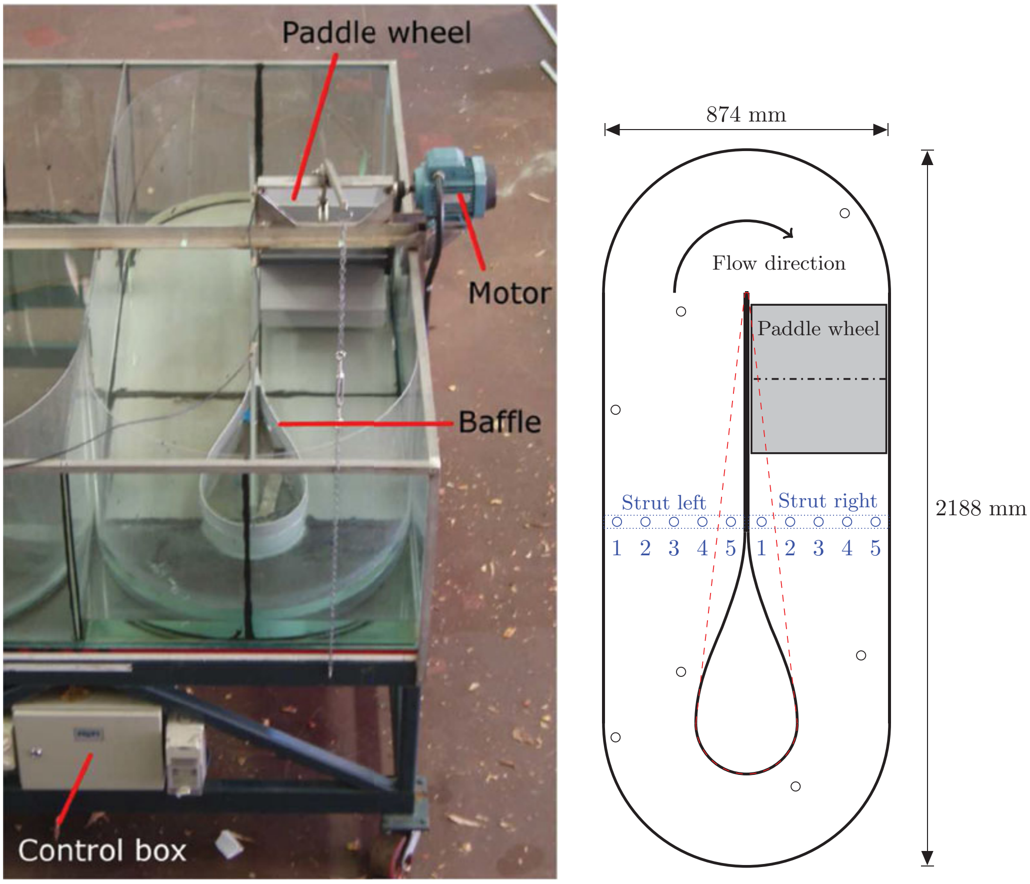

(a) (b)

Fig. 4. (a) Photograph taken from an oblique overhead angle of the experimental raceway pond rig. The paddle wheel can be seen on the right-hand side which was driven by a motor in a direction that circulated fluid clockwise (when viewed from above). The deep end is toward the bottom of the image and there is a section of incline that leads to the shallow end of the tank. An island can be seen that narrows the channel width around one of the turns. An overhead strut (not shown) for holding capsules was attached to the metallic beam of the supporting structure. (b) Diagrammatic overhead view of the raceway pond rig. Some randomly placed mobile capsules have been drawn in the channel. The possible positions for 5 stationary capsules (IDs 1 to 5) placed on an overhead strut (on the left or right) are indicated in blue. The red dotted line is an approximation to the shortest path around the raceway moving at the free surface of the channel. Dimensions indicated are nominal values.

gap during rotation between a blade and the base of the tank was in the order of 5.5 mm. For all experiments reported, the tank was filled with tap water to a height of approximately 120 mm in its deep end ($\sim$100 mm in the shallow end).

In the remainder of this section, a number of experiments using the capsules will be detailed. Since the capsules were only prototypes, the number of trials that could be undertaken was limited with the resources available. However, the work provides a proof-of-concept and illustrates the potential for the flow measurement system to be used in fluid dynamics studies. More extensive studies could be the subject of future research.

Three different examples are provided to illustrate just a few of the potential ways, the capsules can be used. These include lap speed measurements, distributed sensing and streamline flow visualisation through capsule pathlines.

period between reed-switch activations could be measured (and averaged over multiple readings), and the speed of the paddle wheel could be determined. Note the friction caused some variability in the constancy of the motor speed (within a single rotation period and over longer periods of time). In a more extensive study, the motor speed could be monitored throughout a trial to quantify the variability.

https://doi.org/10.1017/S0263574715000041 Published online by Cambridge University Press

Table I. Trial conditions for lap speed measurements.

Trial #	Motor rotational speed, (rpm)	Strut position
1	7	Right
2	7	Left
3	15	Right
4	15	Left
5	20	Right
6	20	Left

3.2. Measuring lap speed from capsule encounter patterns

As a first test application, in this section we illustrate a simple example of how the capsules can be used to quantify the properties of fluid flow. For simplicity, it was decided that the flow near the free surface would be investigated, using stationary capsules (positioned on a strut external to the fluid) and the fluid-mobilised capsules, with the aim of trying to determine the lap speed. The work presented here is an initial study. It is expected that advanced techniques and algorithms will be developed in the future for more comprehensive measurements of the flow velocity (see Section 4).

3.2.1. Method. The mass of each capsule was set to have a nominal value of 9 g. With this weight, the mobile capsules floated in water and had their centres located just below the free surface (∼7 mm). Capsules tended to orient with their optical transmitter/receiver pointing upwards, as a result of their mass distribution, although as they bobbed around and bounced off surfaces, their orientation did fluctuate.

The stationary capsules were placed in holes on a strut suspended (∼94 mm) above the free surface in one of two locations, on the left or right, as indicated in Fig. 4(b). The holes were smaller than a capsule's diameter, so the stationary capsules could be placed with their infra-red receiver and transmitter pointing down, allowing them to communicate with capsules moving below in the fluid. The possible locations for the stationary capsules on the strut can be seen along with the associated capsule ID values. A benefit of using stationary capsules (as opposed to a fixed array of detectors say) is that the system can be easily reconfigured. That is, capsules can be arbitrarily assigned as stationary or mobile and, if stationary, positioned in arbitrary locations. However, a link to a PC for real-time data observation would be useful for a human operator, so a fixed detector may be preferable in some situations.

A total of six experimental trials for the three different rotational speeds of the paddle wheel (namely: ∼7 rpm, ∼15 rpm and ∼20 rpm) and the two possible strut locations (left and right) were conducted. The conditions for the trials are summarised in Table I. In each trial, five capsules were randomly chosen to be stationary and placed on the strut. The remaining seven capsules were designated as mobile to be put into the fluid flow.

Prior to a trial, the capsules designated as stationary were initialised by the control box with ID values 1–5, and put into the *Stationary-Rx* mode (see Section 2.3.1) where they recorded the IDs broadcast by mobile capsules within view. The designated mobile capsules were initialised with ID values 6–12 and put into the *Mobile-Tx-Rx* mode (see Section 2.3.1), and both transmitted their ID and recorded IDs that they sensed from other mobile capsules. As each mobile capsule was initialised, it was dropped into the flow. The stationary capsules were placed into their positions on the overhead strut after all the mobile capsules were in the flow. With all the capsules deployed, the timer value on the control box was then recorded to indicate the time at which data should be considered valid.

3.2.2. Results. During the trials, the fluid-mobilised capsules did laps of the raceway pond, communicating with other mobile capsules and with the stationary capsules as they passed by the overhead strut. The stationary and mobile capsules used their timer to time-stamp (with 0.5 s resolution) when they "saw" another capsule. The maximum number of data points was 200 which was constrained by memory limitations on-board by the microcontroller. To prevent biasing the results, data recorded beyond the time of the first capsule's memory being filled was not included for analysis.

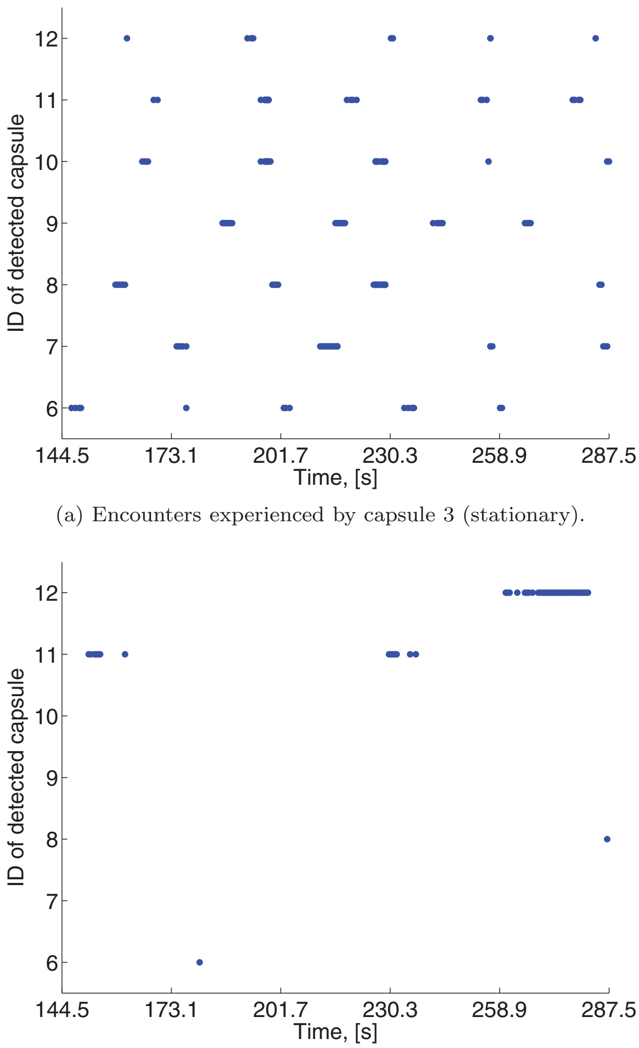

(a) Encounters experienced by capsule 3 (stationary).

(b) Encounters experienced by capsule 7 (mobile).

Fig. 5. Plots showing the encounters experienced by a stationary capsule (ID=3) in (a) and a mobile capsule (ID=7) in (b). The results shown are for trial 1 over an interval where the data is considered valid. Interaction data such as this was obtained for each capsule in each trial. Note some points are superimposed and not temporally resolved due to the limited resolution of the time stamping (0.5 s).

When the capsules passed through the paddle wheel region, they would sometimes move well below the surface, hit the bottom of the tank or be hit by the turning paddle wheel. As the capsules were relatively robust, they were able to function despite the physical knocks they endured.

Figure 5(a) shows an example of the type of data recorded. The encounters experienced by a stationary capsule (ID 3) in trial 1 have been plotted. Each point in the plot indicates an encounter between the stationary capsule in the overhead strut and a mobile capsule passing nearby in the fluid. The data appears to be somewhat periodic as a result of the mobile capsules passing under the strut at somewhat regular intervals as they made laps of the raceway.

Some example of data from the same trial for a mobile capsule (ID 7) has also been plotted and can be seen in Fig. 5(b). In this case, the data is somewhat more sparse since it represents encounters with other mobile capsules moving in the flow, which are more sporadic and occur as capsules that pass each other fleetingly or move alongside each other for a more extended period of time[5]. Figure 5(b) is

[5] Whilst two capsules will communicate most reliably when their IR transmitters/receivers are facing each other, communication is also possible without such alignment provided the capsules are in close proximity. The likely reason for this being that infra-red light is reflected off the capsule shell allowing it to be emitted/received

https://doi.org/10.1017/S0263574715000041 Published online by Cambridge University Press

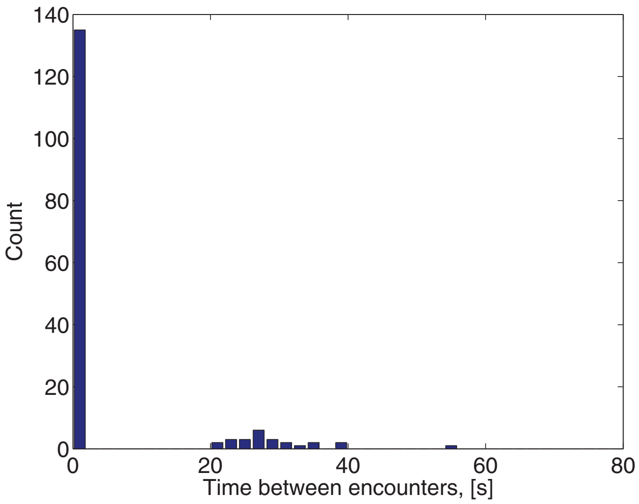

(a) Trial 1 (7 rpm).

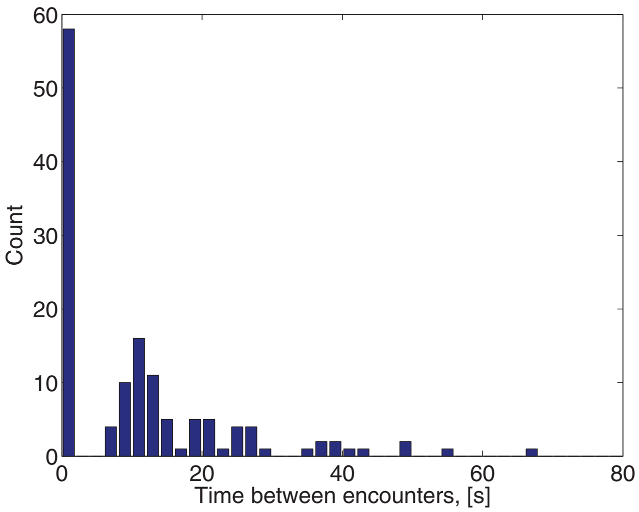

(b) Trial 5 (20 rpm).

Fig. 6. Plots showing the interactions for the stationary capsule 3 in (a) trial 1 (motor rotational speed = 7 rpm) and (b) trial 5 (motor rotational speed = 20 rpm). The relative number of encounters over a short time interval (<2 s) is less for the faster flow rate.

presented for interest's sake only. We do not analyse the data recorded by the mobile capsules here but suggest later how such data might be used in the future work (see Section 4). Note, with an increase in the number of mobile capsules used, we would expect the number of encounters experienced by each mobile capsule to increase.

Data of the kind plotted in Fig. 5 was obtained for all 12 capsules in the 6 trials reported in this section. The data from the stationary capsules (as in Fig. 5(a)) has been analysed in further detail to try and determine the median time for a mobile capsule to circulate a lap of the tank. It was expected that this time could be obtained from the patterns of encounters experienced by the stationary capsules.

Figure 6(a) plots a histogram of the time between encounters using the data shown in Fig. 5(a) for stationary capsule 3 in trial 1 (where the motor rotational speed was 7 rpm). The histogram indicates a large number of closely spaced points over a short time-interval (<2 s), as is observed in Fig. 5(a).

from a wider range of angles. Practically, when two capsules passed each other while moving around the raceway pond, communication was probable.

https://doi.org/10.1017/S0263574715000041 Published online by Cambridge University Press

These closely spaced interactions are due to the fairly large detection zones of the stationary capsules[6], the trajectories and speeds of the mobile capsules, and the communication packet throughput. The relative proportion of these closely spaced encounters is reduced at faster motor speeds (i.e. at higher flow rates) where the capsules pass through the detection zone relatively quickly. This can be seen in Fig. 6(b) which shows the histogram for stationary capsule 3 in trial 5 where the motor rotational speed was 20 rpm.

As we are interested in the lap time (i.e. how long it takes for a mobile capsule to go from the detection zones of stationary capsules, circulate around the tank, and then re-enter the detection zones), in this situation it is not important exactly where the mobile capsules passed under the strut, only that they did pass by. Therefore, we can combine the data from all five stationary capsules to obtain the histograms shown in Fig. 7 (for trials 1–6, respectively)[7].

For clarity, only the longer intervals between encounters (>2 s) have been plotted and used in calculating statistics. It can be seen that in each case there is a peak that corresponds to the most frequent lap time. The peak location and median value of the distribution shifts towards zero as the paddle wheel speed increases[8]. As an example, in Fig. 7(a), the median value is 27.5 s, suggesting this is the median time for a capsule to make a lap of the raceway. While the spread of values evident in the histograms would reflect, in part, the spread of lap times due to different trajectories being taken, some of the spread would be due to stochasticity in the detection process itself (e.g. missed detections, variability in the detection location).

With knowledge of the raceway pond geometry (see Fig. 4(b)), a lower bounds on the median average speed over a lap can be obtained. Assuming motion near the free surface and modelling the capsules as point particles, the shortest path (with length $d_{\min}$) that a mobile capsule can take to make a lap of the raceway can be approximately represented by the red dotted line shown in Fig. 4(b) such that $d_{\min} \approx 3.14$ m. For a median lap time of $\tilde{\tau}$, the median average speed of the capsule over a lap, $\tilde{v}$, is

$$\tilde{v} \geq \frac{d_{\min}}{\tilde{\tau}}. \tag{1}$$

For example, in trial 1 where the median average time to make a lap is $\tilde{\tau} = 27.5$ s, the median average speed of the capsule over a lap is greater than or equal to approximately 0.11 m/s.

Performing this calculation for the data in trials 1–6, we obtain the plot shown in Fig. 8. Note how for the same nominal paddle wheel speed, the results are similar for both locations of the strut suggesting the result is repeatable and independent of strut location. Additional trials could be conducted to model the relationship evident in Fig. 8 for comparison with CFD results.

It is possible to look at the encounters detected for the stationary capsules in a different way. By simply counting the number of encounters experienced by each stationary capsule, it may be possible to determine the most frequent paths taken by capsules passing under the strut. Figures 9(a) and (b) show histograms of the total number of encounters for each stationary capsule in trials 3 and 4, which are for different strut locations but at the same nominal paddle wheel speed of 15 rpm. The results for trial 3 (with the strut on the right) in Fig. 9(a) suggest that after capsules pass through the paddle wheel they tend to be centrally placed in the channel, since the histogram bin count is greatest for capsule 3 located in the centre of the strut. Whereas the results for trial 4 (with the strut on the left) in Fig. 9(b) indicate that capsules tend to be nearer the outer perimeter of the raceway when they pass

[6] Using geometry, the theoretical size of a stationary capsule's detection zone can be calculated. Since, each mobile capsule's IR transmission angle (30 degrees) was smaller than each stationary capsule's IR reception angle (90 degrees), the former would have limited the size of the detection zone (assuming the mobile capsules have their IR LED oriented vertically). For stationary capsules (separated 87 mm apart, and placed on the overhead strut 94 mm above the water), they would have been able to detect the mobile capsules within a circle of radius 25.2 mm at the water surface.

[7] It should be noted that the data obtained from each of the five stationary capsules in a trial was often very similar (especially at lower paddle wheel speeds), because the stationary capsules would detect (almost concurrently) the same mobile capsules passing under the strut. Making the detection zones of the capsules smaller (e.g. moving the strut closer to the free surface) would decorrelate the data.

[8] Here, we are making an assumption (based on human observation) that the capsules are in fact moving around the racetrack and are not simply moving in a recirculation zone under/near the stationary capsules.

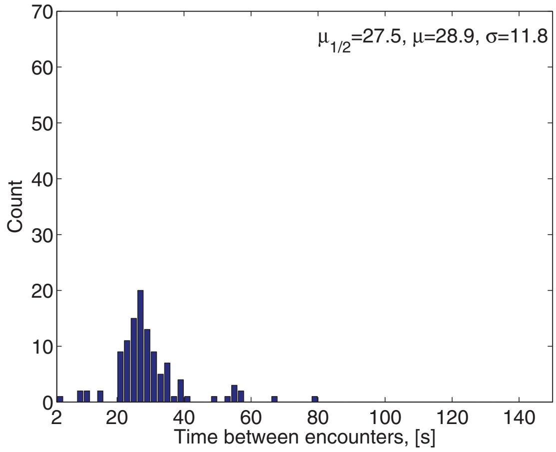

(a) Trial 1 (7 rpm, strut right).

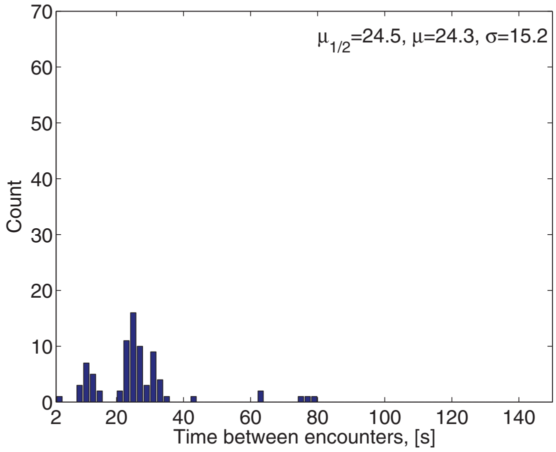

(b) Trial 2 (7 rpm, strut left).

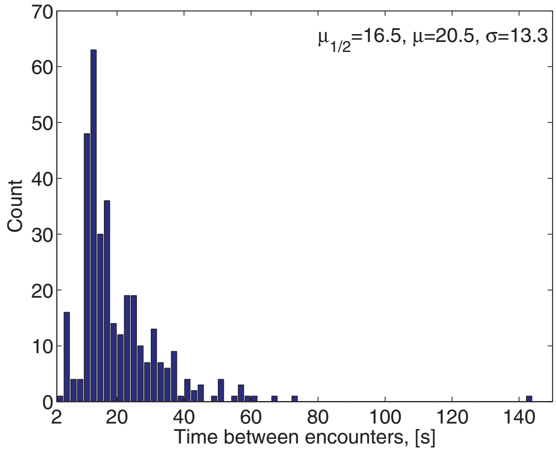

(c) Trial 3 (15 rpm, strut right.)

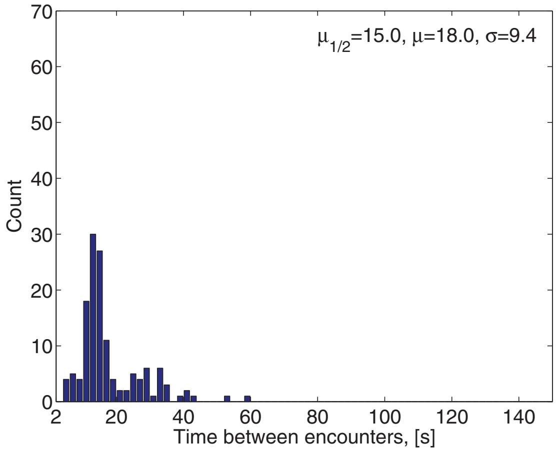

(d) Trial 4 (15 rpm, strut left).

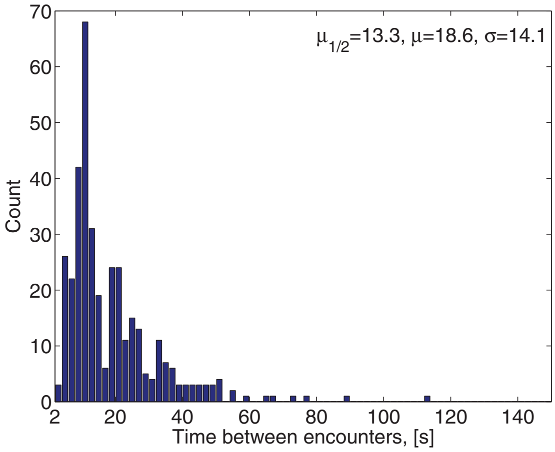

(e) Trial 5 (20 rpm, strut right).

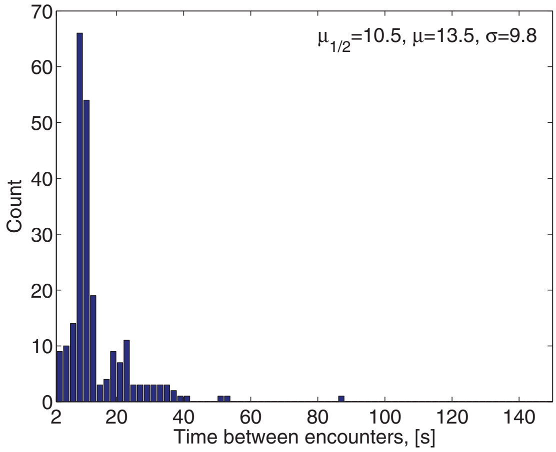

(f) Trial 6 (20 rpm, strut left).

Fig. 7. Histograms showing the time between encounters using the combined data from five stationary capsules.

https://doi.org/10.1017/S0263574715000041 Published online by Cambridge University Press

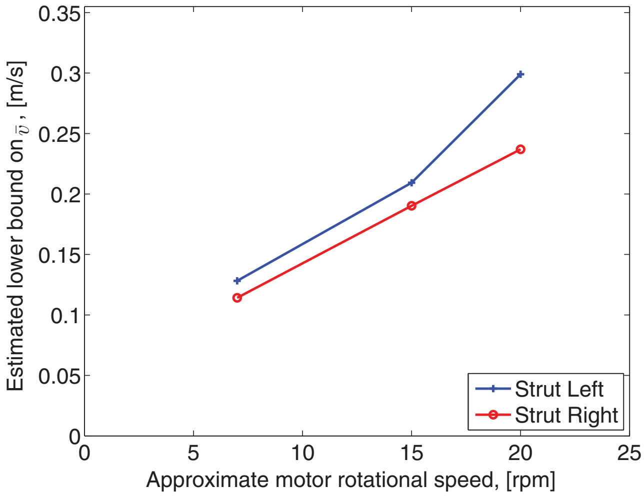

Fig. 8. Lower bounds on the median average speed of a capsule over a lap versus approximate paddle wheel rotational speed. The results depicted were obtained from the data shown in Fig. 7 for trials 1–6.

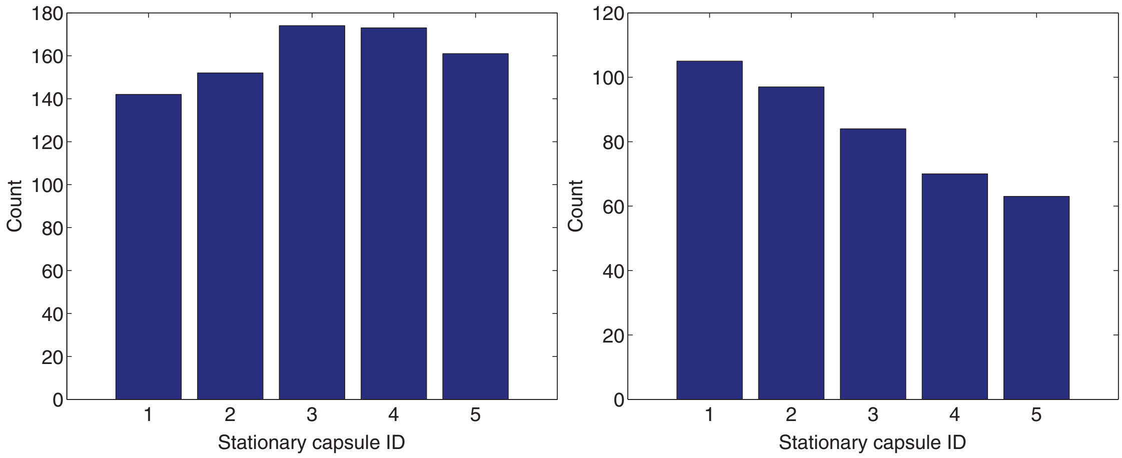

(a) Trial 3 (15 rpm, strut right). (b) Trial 4 (15 rpm, strut left).

Fig. 9. Histograms showing the number of encounters experienced by each of the stationary capsules in trials 3 and 4. The strut positions, right and left for trials 3 and 4 respectively, are indicated in Fig. 4(b).

under the strut. In this case, capsule 1 which was closest to the outer perimeter of the raceway had the largest histogram bin count.

Further work is needed to validate this technique and ensure there is no bias due to unequally sized or overlapping detection regions. However, the preliminary findings indicate the technique is suitable for finding the most frequently traversed paths in a flow[9]. Such results would be useful as they could be compared with data from particle trajectory simulations in CFD modelling.

3.3. Distributed sensing

To demonstrate the capacity for the capsules to be used for distributed sensing within a fluid, a second type of experiment was conducted.

Four capsules were configured in the *Mobile-Sensing* mode (see 2.3.1) in which they each simply recorded measurements from their light sensor. The capsules were weighted to have a nominal weight

[9] There may also be some utility in computing statistics for each individual stationary capsule to explore differences and variability in the encounter rate at different spatial locations. Statistical differences arising from the use of mobile capsules with different properties (e.g. size, density) could also be studied.

https://doi.org/10.1017/S0263574715000041 Published online by Cambridge University Press

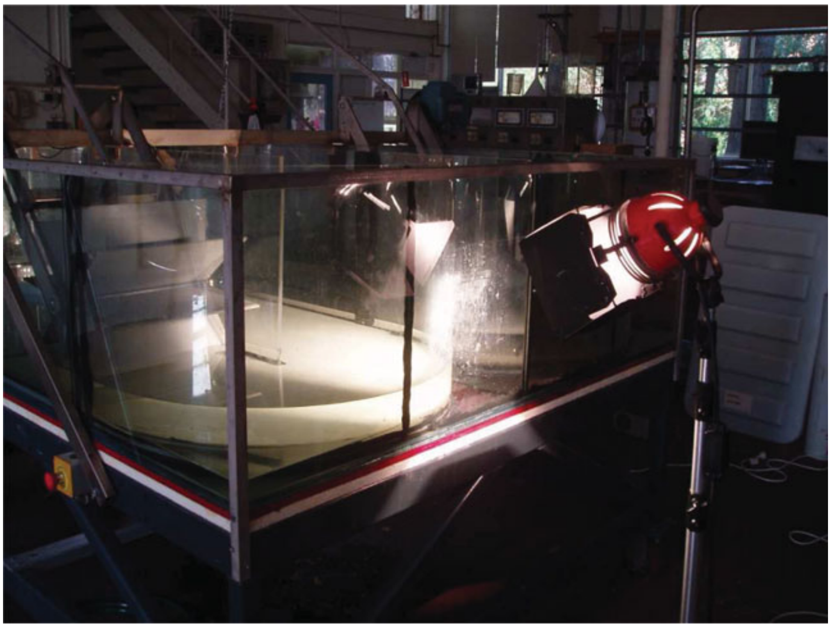

Fig. 10. A flood lamp illuminating part of the raceway pond rig and establishing a light-field gradient along one of the channels.

of 12 g, so they had a density greater than water and tended to be below the free surface during the trial.

The motor speed was set to ∼13 rpm and the capsules were put into the water and allowed to circulate. An external flood lamp was placed so that when switched on it would direct light down the left channel of Fig. 4(b) to create a light-field gradient. The modified set-up can be seen in Fig. 10. The lamp was used to perturb the system. It was manually switched on approximately 79.5 s into the trial and the lamp then remained on until the end of the trial.

Figure 11 shows that prior to the perturbation (when the light was off) each capsule had a relatively high and constant sensor response (note here a high value indicates a low light intensity). After the light was switched on, three of the sensors noticeably responded. Since the capsules were spatially separated, their recorded responses were different. As the capsules moved towards the light source along the light-field gradient, their sensor value dropped (gradually in some instances) as the sensor was illuminated by the light. Fluctuations while moving in the light-field gradient are evident and are likely due to the rotational movement of the capsules (which would have changed the angle of incidence of light on the light sensors or caused the light sensor to be occluded by the other parts inside a capsule) and changes in elevation while moving.

The results in Fig. 11 suggest that the capsule with ID 4, is likely to have made 3 laps of the tank, as there appear to be three distinguishable (i.e. temporally separated) drops in the sensor value. From this, the lap time is of the order of 20 s—a value that is consistent with earlier results (refer to Fig. 8). The light-field gradient is perhaps more evident for capsules 2 and 3 where more gradual declines in sensor values can be seen. The capsule with ID 1 may have had a faulty sensor or may have been stuck in a recirculation zone during the period of data collection (note: human observations were not recorded), as it's sensor value did not change to the same degree as the other sensors. By using multiple capsules however, a *robustness through redundancy* typical of swarm systems can be achieved, so that a faulty sensor does not significantly impair the overall results.

This trial demonstrates how the capsules can perform distributed sensing. Only four capsules were used in this trial due to hardware limitations (such as limited memory for recording), however, a larger scale trial would see many more capsules being used. With capsules located throughout a rig, the onset of a perturbation or event can be temporally localised. Rather than using light sensors, as in this experiment, the capsules could be equipped with chemical sensors and used to measure chemical gradients and determine mixing rates which is useful for some industrial applications. For example, it might be expected that the concentration of a chemical detected by the capsules might be the same

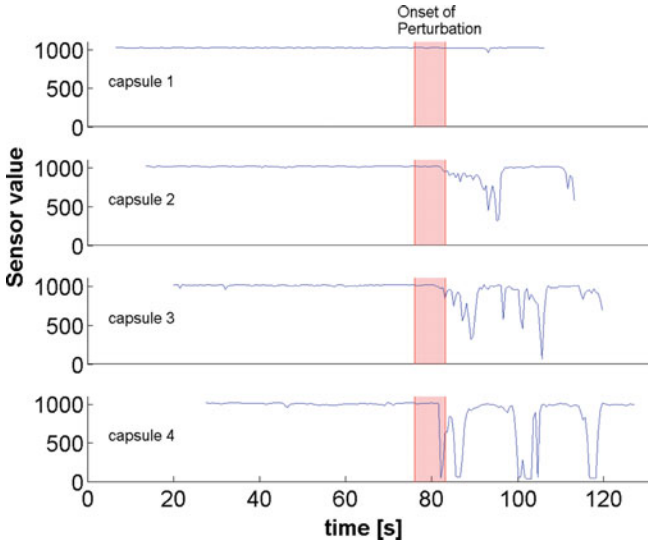

Fig. 11. Example result of distributed sensing by four mobile capsules. A light source was manually switched on approximately 79.5 s into the trial. The light was then kept on for the remainder of the trial. The capsules sensed changes in the light-intensity while they circulated around the raceway pond.

throughout a mixing tank when uniform mixing has been achieved. If 3D positional information were also obtained, events could also be spatially localised (see Section 4 for future work).

3.4. Streamline flow visualisation

The capsules that have been developed can also be used for streamline flow visualisation. Whilst the ultimate aim is for a flow measurement technique that does not require external detection equipment, the current system can be used to directly visualise the fluid flow-lines through the pathlines taken by capsules, simply by using a camera. This is of immediate use to the fluid dynamics research community as it provides a novel way to visualise flow structures not clearly seen before. Additionally, the technique presented here will be of some benefit, since it will allow comparison and validation of results obtained by other capsule measuring techniques.

3.4.1. Methods and results. Ten capsules were each weighted to a nominal mass of 9 g, such that they floated in water. Some capsules with their LEDs on were put into the flow. A camera was mounted above the raceway turn with the island. Photographs of the light-emitting capsules moving in the flow were taken using a 2 s exposure, so that coloured pathlines could be traced out in the resulting images.

The photographs were taken to get multiple capsules in frame simultaneously. Figure 12(a) shows a photograph where five pathlines from five different capsules can be seen. This photograph was taken towards the end of an extended period of testing over which the motor speed, initially set to 15 rpm, decreased to around 11 rpm as a result of friction from prolonged use. The length of each pathline is indicative of the speed. For example, a fast moving capsule will move further in 2 s than a slow moving capsule and will thus have a longer pathline. Standard image processing techniques (including range filtering and skeletonisation) were applied using Matlab to extract the pathlines from the background image. Figure 12(b) shows the result after processing. The length of each pathline was approximately quantified utilising the geodesic distance transform and by performing conversion from pixel units to metres.

Since the photograph exposure time was known, the average speed along each pathline could be calculated. The small red pathline in Fig. 12(a), was created by a capsule moving close to a wall. This capsule had an average speed of $\sim$0.1 m/s ($= \frac{0.2[m]}{2[s]}$). The long orange pathline, which was created by a fast moving capsule near the island, corresponds to a relatively high speed of $\sim$0.25 m/s ($= \frac{0.5[m]}{2[s]}$). The average speed for these pathlines are around the same order of magnitude as the speeds calculated using the encounter rate method (see Fig. 8 in Section 3.2). By combining such results from many photographs it would be possible to construct a planar velocity flow field.

https://doi.org/10.1017/S0263574715000041 Published online by Cambridge University Press

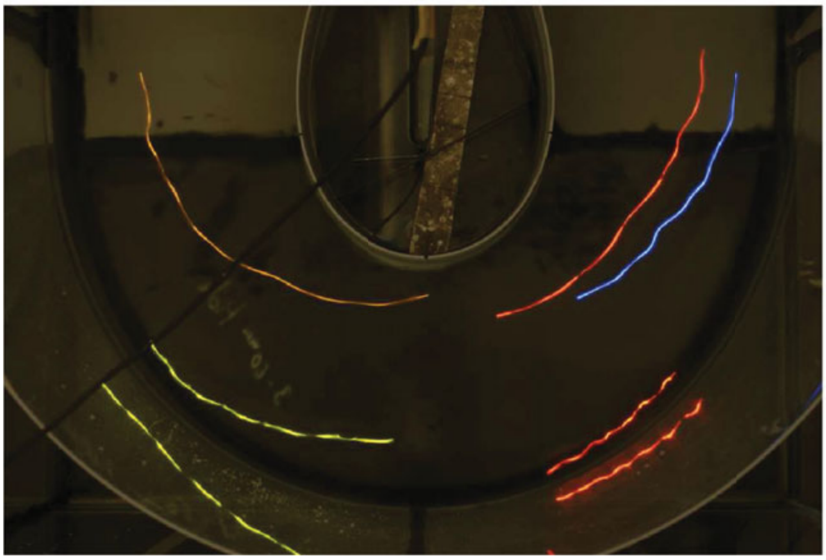

(a)

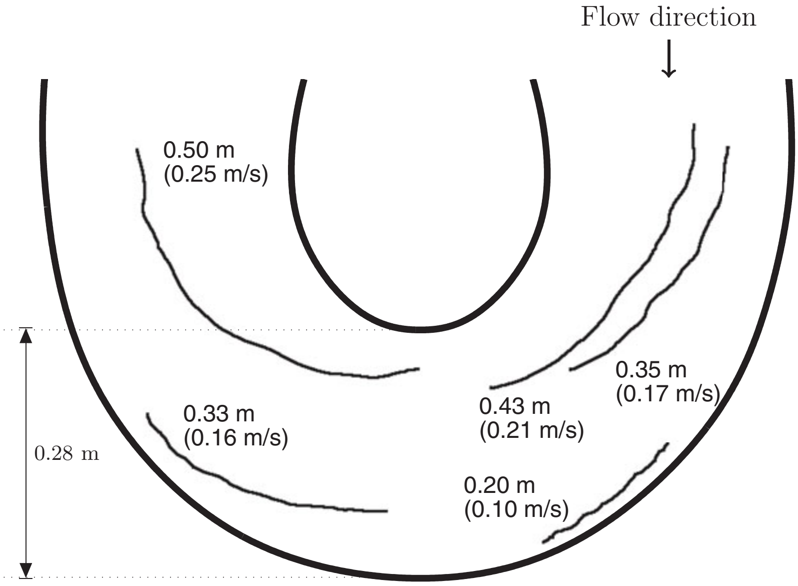

(b)

Fig. 12. (a) Photograph taken with a 2 s exposure. The coloured pathlines that can be seen were created by the movement of individual capsules as they moved in a clockwise direction around a bend. Reflections of pathlines on the tank walls, as well as an overhead cable, are evident in the photograph and should be ignored. (b) Pathlines extracted via image processing with approximate lengths and speeds indicated. Bounding perimeters are shown with thicker lines.

Data of the type shown in Fig. 12 can be used to validate CFD models. As an example, Fig. 13 shows a CFD result obtained for the raceway pond using the transient paddle wheel-driven free surface flow model. See ref. [65] for details describing the fluid flow in a raceway channel. A streamline analysis of the flow field has been performed at one instant in time.

The trajectories of a number of particles have been plotted for seeding locations close to where the capsule pathlines in Fig. 12(a) begin. For illustration purposes, the lengths of the particle trajectories have each been set to be similar to those observed in the practical trial. As can be seen, the CFD particle trajectories appear to be following the same streamlines as the capsules, and the average

https://doi.org/10.1017/S0263574715000041 Published online by Cambridge University Press

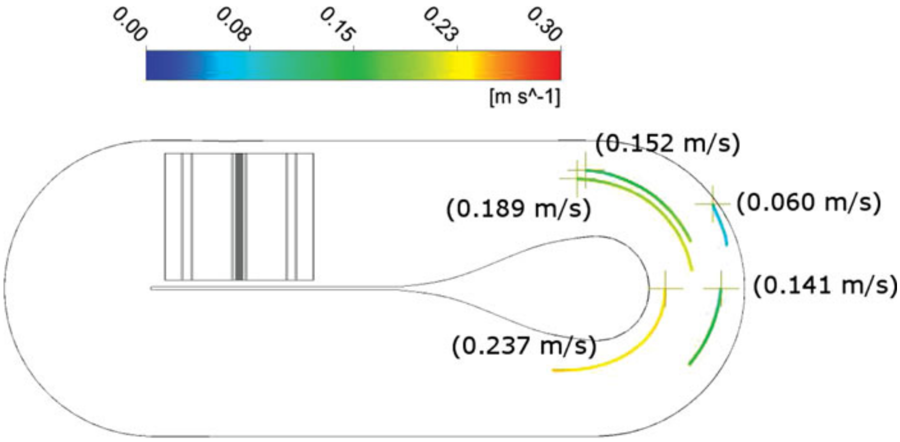

Fig. 13. A CFD result obtained using ANSYS-CFX for a simulation run of the transient paddle wheel-driven free surface model with a paddle wheel speed of 21 rpm and water depth of 75 mm in the deep end. The pathlines of a number of seeded particles are shown and the average speed over each pathline is shown in brackets.

speed over the pathlines appear to be in approximate agreement (while noting slight differences in CFD and experimental model set-ups). The results suggest that the same flow structures are present in both the CFD model and practical set-up. This is promising for the future studies where a more comprehensive CFD validation is required.

Other preliminary work we have conducted (not detailed here) suggests that by programming the capsules, so that they pulse their LEDs on and off cyclically, pathlines can be made smaller and approximately linear such that they can more directly represent a velocity vector field. Using the LEDs allows for easier pathline extraction compared to other possible methods like directly tracking the capsules themselves from frames in video footage. The method also allows ambient lighting to be reduced so that nominally only the capsules are visible allowing the pathlines to be more easily be extracted from the background. Additionally, using different coloured LEDs provides a way of distinguishing between different capsules that may have different properties (weight, size etc.).

The technique detailed in this section provides an inexpensive and simple way to directly visualise the flow patterns in a system, and complements other flow measurement techniques. We expect this technique to be very useful to fluid dynamics researchers. Recently, in collaboration with colleagues, the capsules have proved valuable in providing a unique visualisation of a newly discovered particle clustering phenomenon in mixing tanks.[66]

4. Future Work

The raceway pond case-study demonstrates how the capsules can be used for flow measurement and visualisation as well as distributed sensing. Many avenues have been opened for future work.

In terms of the capsule design, considerable scope exists for reducing the physical size of the capsules. Finer routing could be used for the PCB tracks, and the discrete through-hole components could be replaced by surface mount parts with similar functionality. The ISP header could also be removed, and a bootloader program resident in the microcontroller's memory could be used to allow reprogramming via the infra-red interface. Reducing the size of the main components may be particularly necessary if additional memory (to increase the number of data points that can be stored), or extra functionality is to be added.

To further reduce the size of a capsule, the 20 mm diameter 3V non-rechargeable button cell battery could be replaced with a smaller rechargeable battery (with externally accessible electrodes) or by an alternative means of powering the device. Inductive coupling could be used for non-contact recharging (e.g.[56]), or a solar panel could be incorporated into the design to recharge or power the device externally (e.g.[67]). The capsules could even draw power from the motion of surrounding fluid or if the fluid in a system is an electrolyte, the capsules could potentially contain sacrificial metals in their shells to create a electrochemical cell for generating electrical power.

https://doi.org/10.1017/S0263574715000041 Published online by Cambridge University Press

Whilst the plastic capsule shells used were okay for the prototypes and were capable of withstanding knocks from a paddle wheel or a high speed impeller, as a result they were prone to developing small cracks and leaking. Recently, we have investigated the 3D printing of capsule shells which allows capsule properties (such as size, shell thickness and material) to be tailored to the intended application. This approach is promising and should allow capsules to be reliably deployed into real-life systems (e.g. sewers, pipelines, mixing vessels), where they may be subjected to large vertical drops or high impacts.

At present, an infra-red communication strategy similar to that used in hand-held remote controls has been adopted. Other infra-red communication schemes such as the Infra-red Data Association (IrDA) protocols could be used to achieve a far greater transmission rate if required. For real-life applications (e.g. deployment into sewage systems and industrial flows) where the fluid properties may differ from water, the optical transmission spectrum will need to be considered to ensure infra-red communication is possible. Alternative forms of communication could alternatively/additionally be used, and may be more appropriate for fluids with strong optical attenuation. For example, the capsule shells could act as a conduit for electrical communication (e.g.[68]), or some form of object sensing could be added so capsules know when they have encountered/hit another capsule or object (e.g.[69]).

Currently capsule mobility is provided by the fluid flow. If a form of self-propulsion were added to the capsules, their self-mobility would allow them to autonomously move to places of interest within a system. Additionally, giving the capsules some forms of actuation would facilitate many more applications. For example, robotic capsules in a pipe could coalesce around a leak to seal it off, perform repairs and maintenance, or structural assessment (e.g. see ref. [18]). However, since adding mobility and/or actuators would severely impact the size and power requirements, perhaps a better approach would be to use simple capsule sensors in conjunction with a more sophisticated robot.

An important issue that needs addressing is how best to retrieve the capsules after they have been deployed. For some systems, this can be done with a net or a collection grate (e.g. in a pipeline). In the current system, the capsules were manually removed from the tank after an experiment so data could be extracted, however this approach is somewhat impractical. For closed systems, the capsules could have electromagnets to attach at some collection point where they can be removed. Alternatively, the capsules could be in operation continuously with data being uploaded when they come within range of a data-logging station. Ways of making the capsule shells and electronics from biodegradable materials should also be considered, particularly when the capsules are used in the field and there is a risk of them being lost. Any operational safety issues should also be considered.

If only the pathline visualisation functionality of the capsules is required, then smaller and even simpler capsules could be used, since all that would be required is a LED and a power supply. Something akin to “blinkies” (little encapsulated flashing lights used in entertainment) could be modified for use.

Having demonstrated a proof-of-concept for the capsules, focus can now shift towards developing advanced swarm intelligence algorithms. It is envisaged that mobile-to-stationary and mobile-to-mobile capsule encounters might be used to reconstruct the global flow velocity field. We suspect this may be done by utilising the known identity of capsules and the spatio-temporal constraints imposed by their pattern of encounters, which amounts to solving an inverse problem. This idea could first be investigated in simulation before testing with a physical swarm. Although further study is required, we speculate that the spatial density of the swarm (and resulting encounter rate) will likely impact the maximum spatial and temporal resolution of the system. Benchmarking against a ground truth (e.g. CFD simulations or PIV experiments) will be useful to assess developed methods.

In scaling up the size of the swarm to hundreds or thousands of capsules, various practical issues will need to be considered. A fast way of charging capsule batteries will be needed, along with a means for quickly uploading/downloading data/code. If the spatial density of capsules is too great, interference and the possibility of packet collisions during communication will need to be considered. Issues concerning swarm scalability are discussed in a recent work detailing a self-assembling 1000 robot swarm (one of the largest to date).[70]

Another interesting avenue for investigation that we have been exploring is to look at externally tracking capsules in three dimensions and we have recently developed a vision-based capsule tracking velocimetry (CTV) method. Using a calibrated multi-view set-up, the method allows trajectories of temperature sensing capsules moving in a mixing tank to be recovered from images using triangulation.[71] We have also been able to externally track a pressure sensing capsule in a pipeline rig using a single calibrated camera. The capsule is capable of measuring the pressure along the pipeline which has great potential to the oil/gas industry for pipeline monitoring.

Allowing capsules to self-localise their 3D position appears to be a challenging problem. Using on-board sensors is one possibility, although a solution based on swarm intelligence would be an exciting approach. For example, it should be possible to measure acceleration (and infer position) from capsule encounter rate (e.g. under a high fluid flow velocity gradient, capsules will likely separate and their encounter rate will drop).

Outside of the fluid dynamics, there are a number of other potential applications for the capsules. One possibility is to use the capsules in a health-care setting such as in a hospital. The capsules could be attached to the entrances of different rooms or various objects, and could be used as active markers that communicate with capsules worn by people. Such a system could allow a visually impaired person wearing a capsule to navigate around a capsule-marked building using some audible/tactile feedback, or serve as a memory prompt. The stationary capsule could also record/upload information concerning the status of a patient's health. The interactions (or lack thereof) between patients and other people could also be gathered to determine social influences on health. The capsules could also be used in other areas of swarm robotics research. For example, in collective construction, the capsules could be embedded into the building material and used to encode information required for stigmergy (see ref. [32]).

5. Conclusion

This paper has detailed a group of perceptive communicating capsules for the measurement and visualisation of fluid flow, that will be an inexpensive and easy to use tool for researchers in the field of fluid dynamics. The capsules are individually minimalist and do not possess accelerometers or gyroscopes. Instead, it is through their collective interactions and information gathering effort that measurements of the fluid flow are made.

The capsules have been tested in a small-scale raceway pond set-up where their utility has been demonstrated for measuring the speed of fluid flow, path traversal frequency, and distributed sensing within a fluid. Some of the techniques developed should have immediate use in the study of fluid dynamics and the system provides a basis for many future applications.

The work suggests that by recording encounters between capsules, some global properties of the fluid flow can be elucidated. This is promising, as we work towards the development of more advanced swarm intelligence algorithms for the capsule swarm that focus on the use of mobile-to-mobile capsule interactions in an effort to reconstruct the entire velocity flow field.

Acknowledgement

The authors would like to gratefully acknowledge the support of CSIRO colleagues. Particular thanks to: Kurt Liffman and David Paterson for access to the raceway pond rig and for providing relevant technical information and references; Glen Bradbury, for assistance with the test rig and for useful suggestions; Lawrence Cheung, for photographic expertise and taking a number of the photographs in the paper; Craig Broadley, whose microcontroller development boards provided a platform for early development; Tony Swallow, for advice and guidance with PCB manufacture; Guy Metcalfe for useful discussions and for providing some relevant references; Steven Wang and Chong Wong for useful discussions on applications; Nigel Hoschke for providing feedback on a draft manuscript; and mechanical workshop colleagues for technical assistance and advice. Many thanks also to the three anonymous referees whose constructive comments and suggestions led to improvements in the paper.

References

1. J.-P. Prenel and D. Ambrosini, "Flow visualization and beyond," *Opt. Lasers Eng.* **50**, 1–7 (2012).
2. P. Ball, *Flow, Nature's Patterns, a Tapestry in Three Parts* (Oxford University Press, New York, 2009).
3. R. J. Adrian, "Twenty years of particle image velocimetry," *Exp. Fluids* **39**, 159–169 (2005).

4. J. W. Foreman, Jr., E. W. George and R. D. Lewis, "Measurement of localized flow velocities in gases with a laser Doppler flowmeter," *Appl. Phys. Lett.* **7**, 77–78 (1965).
5. T. D. Dickey, B. Hartman, E. Hurst and S. Isenogle, "Measurment of fluid flow using streak photography," *Am. J. Phys.* **52**, 216–219 (1984).
6. I. D. Šutalo, D. Paterson and M. Rudman, "Flow visualisation and computational prediction in thickener rake models," *Miner. Eng.* **16**, 93–102 (2003).
7. G. Metcalfe, D. Lester, A. Ord, P. Kulkarni, M. Rudman, M. Trefry, B. Hobbs, K. Regenaur-Lieb and J. Morris, "An experimental and theoretical study of the mixing characteristics of a periodically reoriented irrotational flow," *Phil Trans. R. Soc. A* **368**, 2147–2162 (2010).
8. J. C. Gamio, J. Castro, L. Rivera, J. Alamilla, F. Garcia-Nocetti and L. Aguilar, "Visualisation of gasoil two-phase flows in pressurised pipes using electrical capacitance tomography," *Flow Meas. Instrum.* **16**, 129–134 (2005).
9. Y. Takeda, "Velocity profile measurement by ultrasound doppler shift method," *Int. J. Heat Fluid Flow* **7**, 313–318 (1986).
10. B. Warneke, M. Last, B. Liebowitz and K. S. J. Pister, "Smart dust: Communicating with a cubic-millimeter computer," *Computer* **34**, 44–51 (2001).
11. T. Wark, W. Hu, P. Corke, J. Hodge, A. Keto, B. Mackey, G. Foley, P. Sikka and M. Brünig, "Springbrook: Challenges in Developing a Long-Term, Rainforest Wireless Sensor Network," *Proceedings of ISSNIP 2008 International Conference on Intelligent Sensors, Sensor Networks and Information Processing*, Sydney, Australia (2008) pp. 599–604.
12. I. Stoianov, L. Nachman, S. Madden and T. Tokmouline, "PIPENET: A Wireless Sensor Network for Pipeline Monitoring," *Proceedings of the 6th International Symposium on Information Processing in Sensor Networks (IPSN)* Cambridge, MA, USA (2007) pp. 264–273.
13. R. N. Smith, P. Prentis, K. Langendoen and P. Corke, "Pseudoseeds: Investigating Long-Distance, Ocean Seed Dispersal with Wireless Sensors," *Proceedings of 2011 IEEE/RSJ International Conference on Intelligent Robots and Systems (IROS), Workshop on Robotic Environmental Monitoring*, San Francisco, CA, USA (2011).
14. T. Wark, P. Corke, P. Sikka, L. Klingbeil, Y. Guo, C. Crossman, P. Valencia, D. Swain and G. Bishop-Hurley, "Transforming agriculture through pervasive wireless sensor networks," *Pervasive Comput.* **6**(2), 50–57 (2007).
15. M. Hedley, N. Hoschke, M. Johnson, C. Lewis, A. Murdoch, D. Price, M. Prokopenko, A. Scott, P. Wang and A. Farmer, "Sensor Network for Structural Health Monitoring," *Proceedings of the 2004 Intelligent Sensors, Sensor Networks and Information Processing Conference (ISSNIP)*, Melbourne, Australia (2004) pp. 361–366.
16. C. Ramos, J. C. Augusto and D. Shapiro, "Ambient intelligence – the next step for artificial intelligence," *IEEE Intell. Syst.* **23**(2), 15–18 (2008).
17. D. Ding, R. A. Cooper, P. F. Pasquina and L. Fici-Pasquina, "Sensor technology for smart homes," *Maturitas* **69**, 131–136 (2011).
18. N. Correll and A. Martinoli, "Multirobot inspection of industrial machinery," *IEEE Robot. Autom. Mag.* **16**, 103–112 (2009).
19. P. Baronti, P. Pillai, V. W. C. Chook, S. Chessa, A. Gotta and Y. F. Hu, "Wireless sensor networks: A survey on the state of the art and the 802.15.4 and ZigBee standards," *Comput. Commun.* **30**, 1655–1695 (2007).
20. B. Kusy, C. Richter, W. Hu, M. Afanasyev, R. Jurdak, M. Brünig, D. Abbott, C. Huynh and D. Ostry, "Radio Diversity for Reliable Communication in WSNs," *Proceedings of the 10th ACM/IEEE International Conference on Information Processing in Sensor Networks (IPSN)* Chicago, IL, USA (2011) pp. 270–281.
21. J. Yick, B. Mukherjee and D. Ghosal, "Wireless sensor network survey," *Comput. Networks* **52**, 2292–2330 (2008).
22. W. Hu, P. Corke, W. C. Shih and L. Overs, "secFleck: A Public Key Technology Platform for Wireless Sensor Networks," *Proceedings of the 6th European Conference of Wireless Sensor Networks (EWSN)* Cork, Ireland (2009) pp. 296–311.
23. T. Fukuda and S. Nakagawa, "Approach to the dynamically reconfigurable robotic system," *J. Intell. Robot. Syst.* **1**, 55–72 (1988).
24. A. Kamimura, H. Kurokawa, E. Yoshida, S. Murata, K. Tomita and S. Kokaji, "Automatic locomotion design and experiments for a modular robotic system," *IEEE/ASME Trans. Mechatronics* **10**, 314–325 (2005).
25. D. Brandt and D. J. Christensen, "A New Meta-Module for Controlling Large Sheets of ATRON Modules," *Proceedings of the 2007 IEEE/RSJ International Conference on Intelligent Robots and Systems (IROS)* San Diego, CA, USA (2007) pp. 2375–2380.
26. K. Gilpin, A. Knaian and D. Rus, "Robot Pebbles: One Centimeter Modules for Programmable Matter through Self-Disassembly," *Proceedings of the 2010 IEEE International Conference on Robotics and Automation (ICRA)* Anchorage, AK, USA (2010) pp. 2485–2492.
27. J. Bishop, S. Burden, E. Klavins, R. Kreisberg, W. Malone, N. Napp and T. Nguyen, "Programmable Parts: A Demonstration of the Grammatical Approach to Self-Organization," *Proceedings of the 2005 IEEE/RSJ International Conference on Intelligent Robots and Systems (IROS)* Edmonton, Canada (2005) pp. 3684–3691.

28. M. T. Tolley and H. Lipson, "Programmable 3D Stochastic Fluidic Assembly of cm-Scale Modules," *Proceedings of the 2011 IEEE/RSJ International Conference on Intelligent Robots and Systems (IROS)* San Francisco, CA, USA (2011) pp. 4366–4371.
29. E. Bonabeau, M. Dorigo and G. Theraulaz, *Swarm Intelligence: From Natural to Artificial Systems* (Oxford University Press, New York, 1999).
30. C. R. Kube and H. Zhang, "Task modelling in collective robotics," *Auton. Robots* **4**, 53–72 (1997).
31. M. J. B. Krieger and J.-B. Billeter, "The call of duty: Self-organised task allocation in a population of up to twelve mobile robots," *Robot. Auton. Syst.* **30**, 65–84 (2000).
32. R. L. Stewart, "A Stigmergy Rule set Compiler for Collective Construction using the Distance Transform," *Proceedings of IROS 2009 Workshop on Biologically-Inspired Robotics*, St. Louis, MO, USA (2009) pp. 69–76.
33. K. Petersen, R. Nagpal and J. Werfel, "TERMES: An Autonomous Robotic System for Three-Dimensional Collective Construction," *Proceedings of Robotics: Science and Systems VII*, Los Angeles, CA, USA (2011) pp. 257–264.
34. T. A. Phan and R. A. Russell, "An Effective Collaboration Algorithm for Swarm Robots Communicating by Sematectonic Stigmergy," *Proceedings of the 2010 11th International Conference on Control, Automation, Robotics and Vision (ICARCV)* Singapore (2010) pp. 390–397.
35. F. Mondada, G. C. Pettinaro, A. Guignard, I. W. Kwee, D. Floreano, J.-L. Deneubourg, S. Nolfi, L. M. Gambardella and M. Dorigo, "Swarm-bot: A new distributed robotic concept," *Auton. Robots* **17**, 193–221 (2004).
36. R. L. Stewart and R. A. Russell, "A distributed feedback mechanism to regulate wall construction by a robotic swarm," *Adapt. Behav.* **14**, 21–51 (2006).
37. E. Şahin and N. R. Franks, "Measurement of Space: From Ants to Robots," *Proceedings of WGW 2002: EPSRC/BBSRC International Workshop Biologically-Inspired Robotics: The Legacy of W. Grey Walter* Bristol, UK (2002) pp. 241–247.
38. E. Şahin, S. Girgin and E. Uğur, "Area measurement of large closed regions with a mobile robot," *Auton. Robots* **21**, 255–266 (2006).
39. J. A. Rothermich, M. Ihsan Ecemiş and P. Gaudiano, "Distributed Localization and Mapping with a Robotic Swarm," *Proceedings of the Swarm Robotics SAB 2004 International Workshop,* Santa Monica, CA, USA (July 17, 2004), Revised selected papers, Lecture Notes in Computer Science (LNCS) (E. Şahin and W. M. Spears, eds.) (Springer-Verlag, Berlin, 2005), vol. 3342, pp. 58–69.
40. Àlvaro Gutiérrez, A. Campo, F. C. Santos, C. Pinciroli and M. Dorigo, "Social Odometry in Populations of Autonomous Robots," *Proceedings of the Ant Colony Optimization and Swarm Intelligence*, Lecture Notes in Computer Science (LNCS) (M. Dorigo, M. Birattari, C. Blum, M. Clerc, T. Stützle and A. F. T. Winfield, eds.) (Springer-Verlag, Berlin, 2008), vol. 5217, pp. 371–378.
41. C. A. Parker and H. Zhang, "Collective unary decision-making by decentralized multiple-robot systems applied to the task-sequencing problem," *Swarm Intell.* **4**, 199–220 (2010).
42. H. Yu, C.-M. Tang and R. Bashirullah, "An Asymmetric RF Tagging IC for Ingestible Medication Compliance Capsules," *Proceedings of the 2009 IEEE Radio Frequency Integrated Circuits Symposium (RFIC)* Boston, MA, USA (2009) pp. 101–104.
43. P. R. Troyk, "Injectable electronic identification, monitoring and stimulation systems," *Annu. Rev. Biomed. Eng.* **1**, 177–209 (1999).
44. B. Watson, J. Friend and L. Yeo, "Modelling and testing of a piezoelectric ultrasonic micro-motor suitable for *in vivo* micro-robotic applications," *J. Micromech. Microeng.* **20**, 115018 (2010).
45. Z. Nagy, R. Oung, J. J. Abbott and B. J. Nelson, "Experimental Investigation of Magnetic Self-Assembly for Swallowable Modular Robots," *Proceedings of the 2008 IEEE/RSJ International Conference on Intelligent Robots and Systems (IROS)* Nice, France (2008) pp. 1915–1920.
46. P. Dario, C. Stefanini and A. Menciassi, "Modeling and Experiments on a Legged Microrobot Locomoting in a Tubular, Compliant and Slippery Environment," *Experimental Robotics IX*, Springer Tracts in Advanced Robotics (M. H. A. Jr. and O. Khatib, eds.) (Springer-Verlag, Berlin, 2006), vol. 21, pp. 165–174.
47. G. Kósa, P. Jakab, N. Hata, F. Jólesz, Z. Neubach, M. Shoham, M. Zaaroor and G. Székely, "Flagellar Swimming for Medical Micro Robots: Theory, Experiments and Application," *Proceedings of the 2nd Biennial IEEE/RAS-EMBS International Conference on Biomedical Robotics and Biomechatronics (BioRob)* Scottsdale, AZ, USA (2008) pp. 258–263.
48. F. Carpi, N. Kastelein, M. Talcott and C. Pappone, "Magnetically controllable gastrointestinal steering of video capsules," *IEEE/ASME Trans. Biomed. Eng.* **58**, 231–234 (2011).
49. A. A. G. Requicha, "Nanorobots, nems and nanoassembly," *Proc. IEEE* **91**, 1922–1933 (2003).
50. P. Corke, C. Detweiler, M. Dunbabin, M. Hamilton, D. Rus and I. Vasilescu, "Experiments with Underwater Robot Localization and Tracking," *Proceedings of the 2007 IEEE International Conference on Robotics and Automation (ICRA)* Roma, Italy (2007) pp. 4556–4561.
51. J. Das, F. Py, T. Maughan, T. OReilly, M. Messié, J. Ryan, G. S. Sukhatme and K. Rajan, "Coordinated sampling of dynamic oceanographic features with underwater vehicles and drifters," *Int. J. Robot. Res.* **31**, 626–646 (2012).
52. Y. Zhang and J. G. Bellingham, "An efficient method of selecting ocean observing locations for capturing the leading modes and reconstructing the full field," *J. Geophys. Res.* **113**, C04005 (2008).
53. G. Benelli, A. Pozzebon, G. Raguseo, D. Bertoni and G. Sarti, "An RFID Based System for the Underwater Tracking of Pebbles on Artificial Coarse Beaches," *Proceedings of the 3rd International Conference on Sensor Technologies and Applications* Athens, Greece (2009) pp. 294–299.

54. T. T.-T. Lai, W.-J. Chen, K.-H. Li, P. Huang and H.-H. Chu, "TriopusNet: Automating Wireless Sensor Network Deployment and Replacement in Pipeline Monitoring," *Proceedings of the 11th ACM/IEEE International Conference on Information Processing in Sensor Networks (IPSN)* Beijing, China (2012) pp. 61–71.
55. N. Kularatna, C. Wijeratne and B. Melville, "Mixed Signal Approach for Rapid Prototyping of a Compact Smart Pebble for Sediment Transport Monitoring in River Beds," *Proceedings of 2005 IEEE Sensors*, Irvine, CA, USA (2005) pp. 1128–1132.
56. D. K. Abeywardana, A. P. Hu and N. Kularatna, "Design Enhancements of the Smart Sediment Particle for Riverbed Transport Monitoring," *Proceedings of the 4th IEEE Conference on Industrial Electronics and Applications (ICIEA)* Xi'an, China (2009) pp. 336–341.
57. D. M. Gordon and N. J. Mehdiabadi, "Encounter rate and task allocation in harvester ants," *Behav. Ecology Sociobiol.* **45**, 370–377 (1999).
58. M. J. Greene and D. M. Gordon, "Interaction rate informs harvester ant task decisions," *Behav. Ecology* **18**, 451–455 (2007).
59. S. C. Pratt, "Quorum sensing by encounter rates in the ant *Temnothorax albipennis*," *Behav. Ecology* **16**, 488–496 (2005).
60. R. L. Jeanne, "Group Size, Productivity, and Information Flow in Social Wasps," **In**: *Information Processing in Social Insects* (C. Detrain, J.-L. Deneubourg and J. Pasteels, eds.) (Birkhäuser Verlag, Basel, Switzerland, 1999).
61. Atmel Corporation, *AVR410: RC5 IR Remote Control Receiver* (2002) application note.
62. Atmel Corporation, *AVR415: RC5 IR Remote Control Transmitter* (2003) application note.
63. D. A. Paterson, P. Bandopadhayay and K. Liffman, "Design of Energy-Efficient Algal Ponds," *Proceedings of Chemeca 2010: Engineering at the Edge*, Adelaide, Australia (2010) pp. 411–420.
64. P. K. Campbell, T. Beer and D. Batten, "Life cycle assessment of biodiesel production from microalgae in ponds," *Bioresource Technol.* **102**, 50–56 (2011).
65. K. Liffman, D. A. Paterson, P. Liovic and P. Bandopadhayay, "Comparing the energy efficiency of different high rate algal raceway pond designs using computational fluid dynamics," *Chem. Eng. Res. Des.* **91**, 221–226 (2013).
66. S. Wang, G. Metcalfe, R. L. Stewart, J. Wu, N. Ohmura, X. Feng, and C. Yang, "Solid-liquid separation by particle-flow-instability," *Energy and Environmental Science*, **7**(12), pp. 3982–3988 (2014).
67. G. M. Tina, V. Cristina, A. Paolo, P. Luca, G. A. Dario and P. Massimo, "Design Considerations about a Photovoltaic Power System to Supply a Mobile Robot," *Proceedings of the 2010 IEEE International Symposium on Industrial Electronics (ISIE)* Bari, Italy (2010) pp. 1829–1834.
68. A. Silvola and R. A. Russell, "Robot Communication via Substrate Vibrations," *Proceedings of the 2005 Australasian Conference on Robotics and Automation (ACRA)* Sydney, Australia (2005) pp. 239–244.
69. S. Mintchev, C. Stefanini, A. Girin, S. Marrazza, S. Orofino, V. Lebastard, L. Manfredi, P. Dario and F. Boyer, "An Underwater Reconfigurable Robot with Bioinspired Electric Sense," *Proceedings of the 2012 IEEE International Conference on Robotics and Automation (ICRA)* Saint Paul, MN, USA (2012) pp. 1149–1154.
70. M. Rubenstein, A. Cornejo and R. Nagpal, "Programmable self-assembly in a thousand-robot swarm," *Science* **345**, 795–799 (2014).
71. R. L. Stewart, I. D. Šutalo, and C. Y. Wong, "Three-dimensional tracking of sensor capsules mobilised by fluid flow," *Measurement Science and Technology* (accepted for publication) (2015).